Pure Appl. Chem., Vol. 85, No. 2, pp. 437–451, 2013.
http://dx.doi.org/10.1351/PAC-CON-12-08-17

Metal nanoparticles for energy conversion*

Naoki Toshima

Department of Applied Chemistry, Tokyo University of Science Yamaguchi, SanyoOnoda, Yamaguchi 756-0884, Japan

Abstract: Energy has emerged as a strategic priority not only in research but also in all aspects of human lives. Most worldwide problems could be solved if energy were plentiful. In order to solve the energy problem, the following methods could be applicable: the creation of electricity from renewable energy resources, increase in conversion efficiency from fossil fuels to electricity, recovery of electricity from exhaust heat energy, and reduction of energy consumption. Nanotechnologies have already shown good promise in addressing and offering solutions in these priority areas. Here, we have demonstrated the application of metal nanoparticles (NPs) to electrocatalysts for the polyelectrolyte fuel cell (increase in conversion efficiency) and to additives to form hybrids with organic thermoelectric materials of conducting polymers (recovery of energy from exhaust heat). Thus, Pt monometallic and AuPt bimetallic NPs were used for electrocatalysts with high performance, and Pt and Au NPs were applied to hybrid thermoelectric materials to fabricate hybrid films with increasing thermoelectric performance for conversion of the exhaust heat near room temperature.

Keywords: conducting polymers; electrocatalysts; fuel cells; gold; metal nanoparticles; organic thermoelectric materials; platinum.

INTRODUCTION

Metal nanoparticles (NPs) have received much attention not only from academia but also from industry because of their wide variety of applications such as catalysts, photonics, electronics, magnetism, sensors, and biomedicals [1–3]. In fact, the number of publications on applications of NPs is increasing rapidly as shown in Fig. 1 based on the data by SciFinder®. On the other hand, the energy problem is the most important issue for human beings, because most of the problems in the world concerning food, water, electricity, and the environment would be solved if plentiful energy could be supplied [4,5]. In addition, most energy cannot be used directly for the original purpose. About two-thirds of the fossil energy is exhausted as heat energy without utilization. Thus, the improvement of the conversion efficiency of chemical energy to electric energy and recovering of exhausted heat energy as electric energy could be very important for human beings. On the basis of these backgrounds, we present here the application of metal NPs to electrocatalysts for fuel cells, which directly convert chemical energy to electricity [6–8], and to hybrid thermoelectric materials, which can convert exhaust heat energy to electricity [9–13].

Pure Appl. Chem.* **85, 315–462 (2013). A collection of invited papers based on presentations at the 12th Eurasia Conference on Chemical Sciences, Corfu, Greece, 16–21 April 2012.

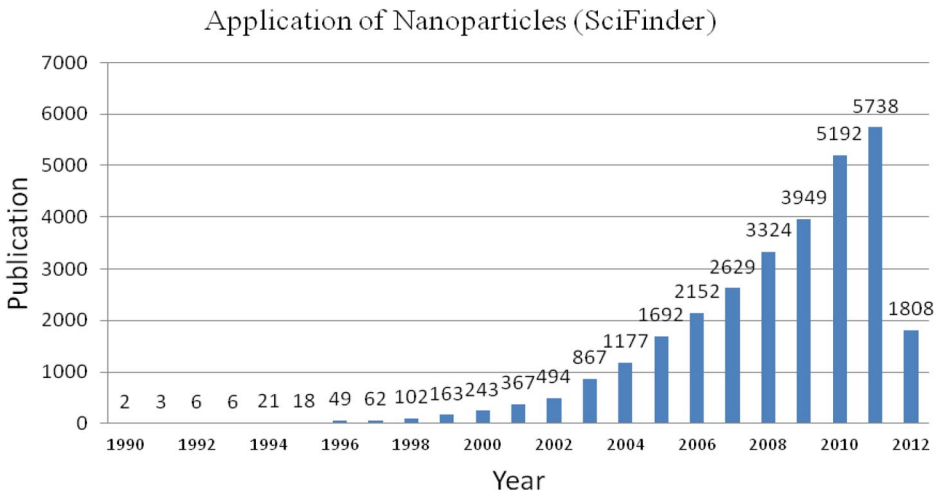

Fig. 1 Number of publications on applications of NPs in each year since 1990 from SciFinder.

ELECTROCATALYSTS FOR FUEL CELLS

Background and motivation

Fuel cells can directly convert chemical energy into electricity with high efficiency, 40–60 %. Although several types of fuel cells are the subject of research and development, we are rather interested in a polymer electrolyte membrane fuel cell, which is usually operated at 50–100 °C by using perfluorinated sulfonic acid (PFSA) copolymer, e.g., Nafion®, as the common electrolyte (Fig. 2) [7]. The polyelectrolyte fuel cells are expected to be applied to a back-up power, potable power, specialty vehicles, distributed power generation, and transportation. The advantages of polyelectrolyte fuel cells are that they have no problems in corrosion and electrolyte management due to solid electrolyte, can be operated at rather low temperature, and provide quick start-up. The disadvantages include the fact that catalysts are expensive and sensitive to fuel impurities [14–17], and the membranes are operated only at low temperature [18]. The former disadvantage can be overcome by improving the catalyst. Thus, we have tried to improve the catalyst for the reduction of Pt consumption. This could be the most important problem which should be solved to develop the practical polyelectrolyte fuel cell. For this purpose, polymer-protected Pt NPs have been developed at first as the electrocatalyst of the fuel cell instead of carbon-supported Pt catalysts, in which half of the surface atoms of Pt particles are covered by the support and cannot be used as the effective catalyst. Secondly, core/shell-structured bimetallic NPs with a Pt shell were prepared [19,20]. In this method, Pt atoms were used only on the surface of the catalyst particles. Thus, instead of supported Pt catalysts, polymer-protected Pt NP catalysts were prepared without inorganic supports. Poly(*N*-vinyl-2-pyrrolidone) (PVP) is often used to protect metal NPs. However, PVP is known as an insulating polymer. Thus, instead of PVP, we used PFSA copolymer, which is the polyelectrolyte or ionomer of the fuel cell and has a high ionic conductivity. Thus, we successfully used only a small amount of PFSA to protect Pt NPs [21].

Experimental

Preparation of PFSA-protected Pt nanoparticles

Pt NPs protected by PFSA were prepared from hydrogen hexachloroplatinate(IV) hexahydrate (Wako Pure Chemical Industries) and Nafion DE1020CS PFSA dispersion (DuPont Fuel Cells). A fixed volume of PFSA (R = 5–0.005) was mixed with Milli-Q water and hydrogen hexachloroplatinate(IV).

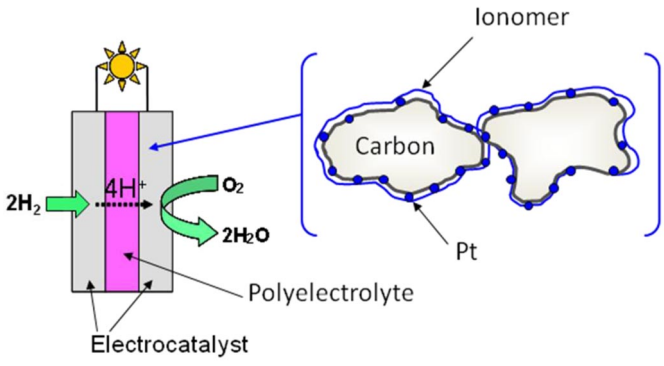

Fig. 2 Concept of a polyelectrolyte fuel cell.

R denotes a molar ratio of monomer unit of PFSA to Pt ions. The Pt ions were reduced by sodium tetrahydroborate. (Five times moles of $NaBH_4$ were used.) The produced Pt NPs were purified and concentrated by ultrafiltration under Ar at pressure of 1.20–1.01 kg cm^{-2} with an ultrafilter (Advantec, Q0100076E) and washed with Milli-Q water several times until chloride ion was not detected in a filtrate solution. Finally, the dispersion of the PFSA-protected Pt (Pt/PFSA) NPs was concentrated to 5–10 wt % Pt content for the electrochemical measurements.

Preparation of PFSA-protected AuPt bimetallic nanoparticles

The AuPt/PFSA NPs were synthesized from hydrogen tetrachloroaurate(III) and hydrogen hexachloroplatinate(IV) hexahydrate and Nafion dispersion by simultaneous reduction. After a fixed volume of the PFSA solution (R = 0.5 %) was mixed with deoxidized Milli-Q water for 30 min, the solutions of hydrogen tetrachloroaurate(III) and hydrogen hexachloroplatinate(IV) hexahydrate were added to the mixture, followed by stirring the solution for 1 h under an atmosphere of nitrogen in the dark. Sodium tetrahydroborate was added to the mixed solution at 0 °C, and then the mixed solution was kept stirring for 1 h at 0 °C. The AuPt/PFSA NPs were purified by filtration with ultrafilter (Advantec, Q0100076E) by washing with Milli-Q water several times until no chloride ions were detected in the filterate.

Characterization and evaluation of PFSA-protected metal nanoparticles as electrocatalysts

UV–vis absorption spectra were measured with a Shimadzu UV-2500PC recording spectrophotometer using a quartz cell with a 10 mm optical path length. Measurements of transmission electron microscope (TEM) image and scanning TEM with energy dispersion X-ray spectrometry (STEM/EDS) were carried out with JEM 2010 and JEM 200F, respectively. The electrochemical (EC) measurements were carried out using a rotating disk electrode (RDE) in an Ar- or O_2-saturated 0.1 mol L^{-1} perchloric acid solution. A conventional three-electrode cell was equipped with a reversible hydrogen electrode (RHE) and platinized foil as the reference and counter electrode, respectively. The sample electrodes were prepared by direct dropwise addition of 20 and 3.92 µg platinum of the Pt/PFSA and AuPt/PFSA NPs, respectively, onto a rotating electrode surface made of glassy carbon and by drying under N_2 atmosphere. The Pt content in the colloidal solution was analyzed by inductively coupled plasma atomic emission spectrometry (ICP-AES). Commercially available Ketjen black-supported 50 wt % platinum catalyst (Pt/C) was used as a reference catalyst.

Results and discussion

PFSA-protected Pt nanoparticles as the electrocatalysts

PFSA-protected Pt NPs were prepared by two methods, i.e., alcohol reduction [22] and $NaBH_4$ reduction [23,24]. In the alcohol reduction method, the produced Pt NPs had a large particle size and easily formed the aggregates by heating, which were observed by TEM as shown in Fig. 3a. The $NaBH_4$ reduction at 0 °C produced brown-colored dispersions which were composed of PFSA-protected small Pt particles and formed the nanonetwork on TEM grids after ultrafiltration. The TEM photograph is shown in Fig. 3b. The nanonetwork observed in the TEM image suggested that such networks were present even in the dispersions, and also could be formed on the electrode surface when the dispersions were cast on the electrodes of fuel cells. This network formation will be an advantage for the fuel cells because of easy electrical contact among Pt NPs as well as between the Pt NP and the electrode, and in addition because of easy removal of by-produced water from the electrode.

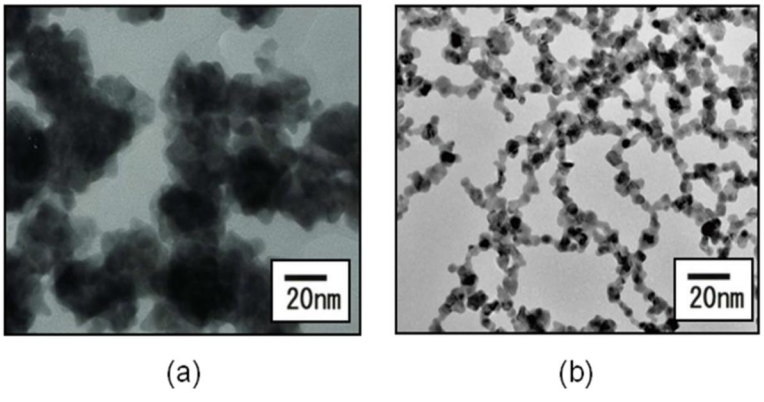

Fig. 3 TEMs of Pt NPs prepared by (a) ethanol (EtOH) reduction and (b) $NaBH_4$ reduction.

EC surface areas of the PFSA-protected Pt NPs prepared by various methods are summarized in Table 1. They vary depending on the preparation method and are smaller than that of the commercial Pt/Ketjen catalyst. In the alcohol reduction method, Pt NPs prepared by reduction with 2-propanol have smaller EC surface area than those prepared by reduction with ethanol (13.3 m^2 g-Pt^{-1}). In the $NaBH_4$ reduction method, Pt NPs before washing with ultrafiltration have small EC surface area, but the washing of Pt NPs with ultrafiltration increases the EC surface area. This increase in surface area coincides with the clear nanonetwork formation after ultrafiltration. The PFSA-protected Pt NPs prepared by $NaBH_4$ reduction and ultrafiltration showed mass activity for oxygen reduction reaction (ORR) at 0.9 V as 191 A g-Pt^{-1}, which was higher than that of the commercial Pt/Ketjen (174 A g-Pt^{-1}), although the EC surface was smaller than that of Pt/Ketjen (32.1 m^2 g-Pt^{-1} and 70.8 m^2 g-Pt, for Pt NPs and Pt/Ketjen, respectively) as shown in Table 1.

Table 1 EC surface area and mass activity for ORR at 0.9 V of PFSA-protected Pt NPs and commercially available Pt/Ketjen.

Sample	EC surface area	Mass activity@0.9V
Pt NPs (EtOH reduction)	13.3 m^2/g-Pt	75.1 A/g-Pt
Pt NPs ($NaBH_4$ reduction before ultrafilitration)	3.7 m^2/g-Pt	13.4 A/g-Pt
Pt NPs ($NaBH_4$ reduction after ultrafilitration)	32.1 m^2/g-Pt	191 A/g-Pt
Pt/Ketjen	70.8 m^2/g-Pt	174 A/g-Pt

PFSA-protected AuPt bimetallic nanoparticles as the electrocatalysts

The catalytic activity of metal NPs is often improved by addition of other elements by forming alloy NPs or so-called core/shell-structured bimetallic NPs [25,26]. In order to reduce the consumption of Pt metal in the electrocatalysts, the bimetallic NPs are required to have a Au-core/Pt-shell structure, since Pt is known as the active element as the electrocatalyst for the fuel cell while Au is an inactive element. The Au-core/Pt-shell-structured AuPt bimetallic NPs were reported to be prepared by alcohol reduction in the presence of PVP [27]. We prepared the AuPt bimetallic NPs in the presence of PFSA instead of PVP by alcohol reduction and by $NaBH_4$ reduction as well.

The products obtained by alcohol reduction were aggregates of AuPt bimetallic NPs, while those by $NaBH_4$ reduction were colloidal dispersions of the bimetallic NPs. UV–vis absorption spectrum of the colloidal dispersion of AuPt bimetallic NPs prepared by $NaBH_4$ reduction at the molar ratio of Au/Pt = 1/4 showed only tailing absorption without any shoulder due to the plasmon peak of Au NPs, indicating the absence of Au NPs and bimetallic NPs covered by Au atoms. The TEM image and histogram of the size distributions of the AuPt bimetallic NPs obtained by $NaBH_4$ reduction before ultrafiltration are shown in Fig. 4a and those after ultrafiltration in Fig. 4b. The treatment of the ultrafiltration promoted the nanonetwork formation by the NPs as clearly illustrated in Fig. 4, although the size of the NPs was kept almost constant. The high-resolution TEM (HR-TEM) images are shown in Fig. 5, indicating that the metal NPs closely contact with each other, but never form a single crystal with a common fringe. Nevertheless, the HR-TEM images support the stronger contact of metal NPs after ultrafiltration than before the ultrafiltration. The SEM photograph of dry film of the PFSA-protected AuPt bimetallic NPs is shown in Fig. 6, which indicates a relatively smooth surface and supports the nanonetwork formation even in the dry state. The same network was realized on SAXS (small-angle X-ray scattering) in the dispersion of the NPs. This nanonetwork may be useful for the removal of by-produced water in the fuel cells as well as the diffusion of source gas. TEM image of the single NP was observed with a spherically aberrated scanning TEM (Cs-STEM), as shown in Fig. 7. The line analysis of elements by EDS indicates that Au and Pt are located rather at the center (core) and

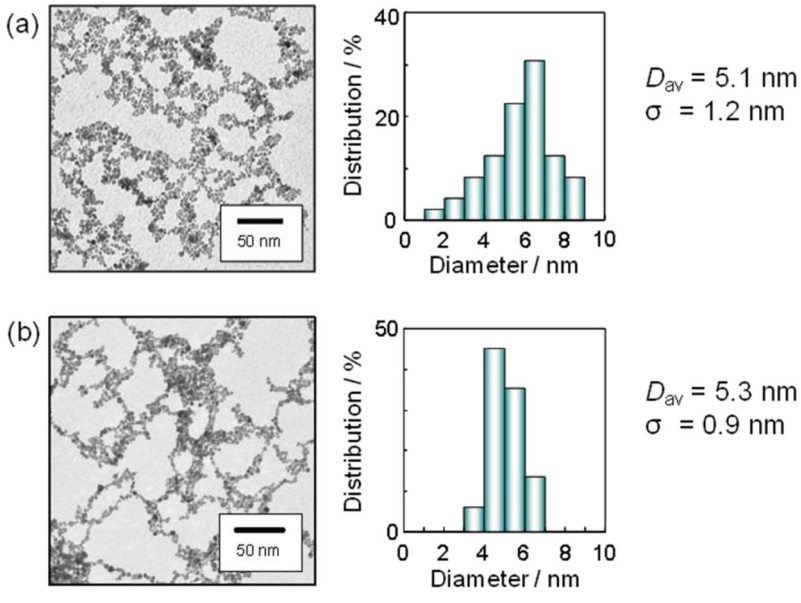

Fig. 4 TEM images and size distribution histograms of PFSA-protected AuPt bimetallic NPs (a) before ultrafiltration and (b) after ultrafiltration.

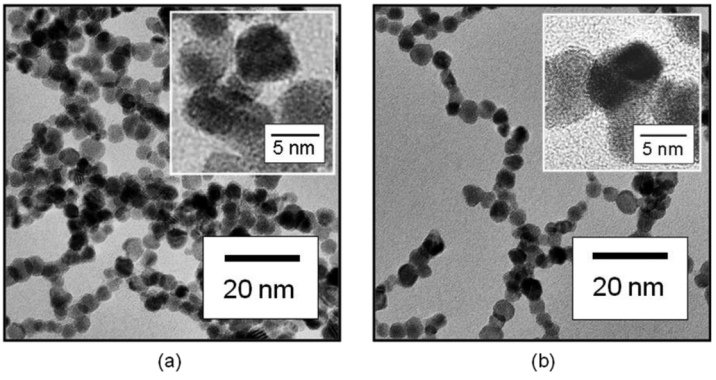

Fig. 5 HR-TEM images of PFSA-protected AuPt bimetallic NPs (a) before ultrafitration and (b) after ultrafiltration.

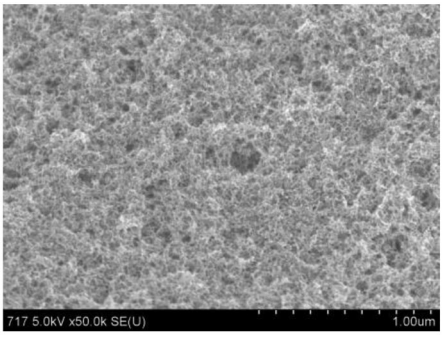

Fig. 6 SEM image of the film cast from dispersions of PFSA-protected AuPt bimetallic NP.

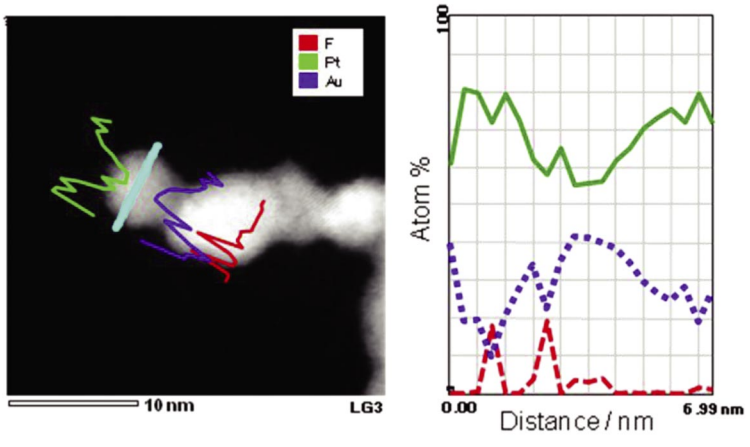

Fig. 7 EDS line analysis of a PFSA-protected AuPt (Au:Pt = 1:4) bimetallic NP. (——, Pt; -----, Au; – – –, F).

near the edge (shell) of the particle, respectively. Thus, the AuPt bimetallic NPs prepared by the present method can be concluded to have a Au-core/Pt-shell structure.

EC surface area and mass activity for ORR were measured for the AuPt bimetallic NPs thus characterized. The results are summarized in Table 2 on comparison with the PFSA-protected Pt NPs

and the commercially available Pt/C catalyst (Pt/Ketijen). The mass activity of AuPt (Au:Pt = 1:4) bimetallic NPs for ORR at 0.9 V is higher than that of the commercial catalyst, although the EC surface area is lower than that of the commercial catalyst.

Table 2 EC surface area and mass activity for ORR or 0.9 V of AuPt bimetallic NPs and the related materials.

Sample	EC surface area	Mass activity@0.9V
PFSA-protected Pt NPs	32.1 m^2/g-Pt	191 A/g-Pt
PFSA-protected AuPt NPs	38.6 m^2/g-Pt	270 A/g-Pt
Pt/Ketjen	70.8 m^2/g-Pt	174 A/g-Pt

Summary of electrocatalysts

Single-nanometer-sized PFSA-protected Pt and AuPt NP catalysts for polyelectrolyte fuel cells were prepared by reduction of the corresponding ions by alcohol reduction and $NaBH_4$ reduction in the presence of PFSA in water. The $NaBH_4$ reduction at 0 °C could give the more favorable dispersion of metal NPs than alcohol reduction in both Pt and AuPt cases. Both NPs formed nanonetworks, especially after ultrafiltration for purification, which should improve the diffusion of source gasses and produced water in catalyst layers. The PFSA-protected AuPt bimetallic NPs prepared by the simultaneous reduction with $NaBH_4$ had a Au-core/Pt-shell structure, which was favorable for reduction of Pt consumption, and had high activity as electrocatalyst. Pt mass activities for ORR of the PFSA-protected Pt and AuPt NPs were observed to be higher than the commercial carbon-supported Pt/Ketjen catalyst. The higher activity of AuPt bimetallic NPs than Pt NPs could be interpreted by the partial electron transfer from Au core to Pt shell [28] because Au atoms are not located on the surface of the electrocatalyst and known as inactive for ORR as the electrocatalyst in spite of the high activity as an oxidation catalyst at low temperature [29]. It should be emphasized that well-dispersed PFSA-protected AuPt bimetallic NPs will have advantages to construct practical membrane electrode assemblies from viewpoints of processing and cost.

ADDITIVES FOR ORGANIC THERMOELECTRIC MATERIALS

Background and motivation

Thermoelectric materials are the materials that can convert the heat energy to the electric energy and vice versa. Thus, thermoelectric materials can be used for the power generation from temperature difference and the electronic cooling by electricity as shown in Fig. 8. Since most of the chemical

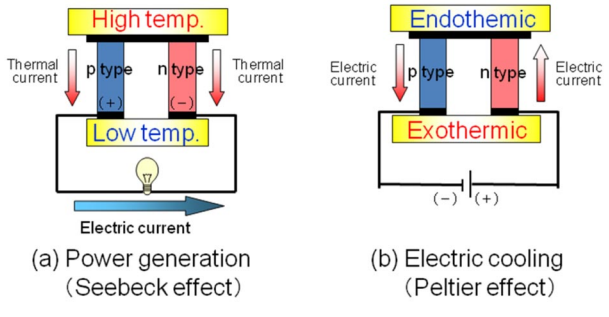

Fig. 8 Schematic illustration of thermoelectric devices for (a) power generation by temperature difference and (b) electronic cooling by electric power.

energy of the fossil fuel is abandoned to the atmosphere as exhaust heat without use, the recovery of the exhaust heat as electric energy by using thermoelectric materials is an interesting and challenging subject [9–13]. However, almost all thermoelectric materials reported were an inorganic semiconductor.

Thermoelectric performance is usually evaluated by dimensionless thermoelectric figure-of-merit ZT, which is defined as the following formula: $ZT = (\sigma S^2/\kappa)\,T$, where σ, S, κ, and T are electrical conductivity, Seebeck coefficient, thermal conductivity, and absolute temperature, respectively. The ZT value of practically used thermoelectric materials Bi_2Te_3 is about 1.0. Thus, $ZT = 1.0$ is often a target to develop new thermoelectric materials.

We have developed organic thermoelectric materials composed of conducting polymers [30–34]. The historical processes are summarized in Table 3. The organic thermoelectric materials have some advantages compared with inorganic ones: plenty of carbon resources, easy synthesis, and easy processing can provide low cost for the production of thermoelectric devices. The low thermal conductivity, low density, and high flexibility of conducting polymers are the essential properties favorable for organic thermoelectric materials. Recently, organic thermoelectric materials with high performance (dimensionless figure-of-merit ZT = 0.25) were reported by controlling the oxidation level of conducting polymers [35]. In addition, the improvement of the thermoelectric performance was reported by using inorganic materials like carbon nanotubes [36] and bismuth telluride NPs [37]. Here we used metal NPs for improving the thermoelectric performance of organic conducting polymers by keeping the advantages of organic materials [38].

Table 3 Thermoelectric properties at room temperature of organic conducting polymers prepared by the author's group.

Cond. Polymer[a] (dopant)[b] (stretching ratio)	σ/S cm^{-1}	S/μV K^{-1}	P/μW m^{-1} K^{-1}	κ/W m^{-1} K^{-1}	ZT/ - (r.t.)
PANi (OA) (–)	2.7–33	10–25	~0.03	(>1)	1×10^{-5}
PANi (PA) (–)	~6	~10	0.06	0.1	2×10^{-4}
PANi (CSA) (–)	188	7	0.9	0.15	2×10^{-3}
Layered PANi (CSA) (–)[c]	173	14	3	0.18	5×10^{-3}
PANi (CSA) (180 %)[d]	260	40	41	0.3	4×10^{-2}
PPy (TSA) (–)	180	11	2	0.2	3×10^{-3}
P(EtOPV-*co*-PV) (I_2) (–)	2.9	41	0.49	0.05	3×10^{-3}
P(EtOPV-*co*-PV) (I_2) (310 %)[e]	350	47	74	0.25	1×10^{-1}

[a]PANi: polyaniline, PPy: polypyrrole, P(EtOPV-*co*-PV): copolymer of 2.5-diethoxyphenylenevinylene and phenylenevinylene.
[b]OA: oxalic acid, PA: phosphoric acid, CSA: (±)-10-camphorsulfonic acid, TSA: *p*-toluenesulfonic acid, I_2: iodine.
[c]Multilayered films of CSA-doped and undoped PANis: H. Yan et al., *Chem. Lett*. 1212 (1999).
[d]H. Yan et al., *Macromol. Mater. Eng*. **286**, 214 (2001).
[e]Y. Hiroshige et al., *Synth. Met*. **157**, 567 (2007).

Experimental

In situ preparation of Au nanoparticles along with polymerization of aniline

Au NPs were prepared in situ along with polymerization of aniline by applying a redox reaction between $HAuCl_4$ and aniline. The redox reaction was carried out by dropwise addition of an aqueous solution of the designed amount of $HAuCl_4$ into 50 mL of 1 mol/L HCl solution containing 50 mmol of purified aniline monomer in a 100-mL flask in an ice bath. After the addition of $HAuCl_4$, an aqueous solution of ammonium peroxodisulfate ($(NH_4)_2S_2O_8$, 62.5 mmol) was dropwise added to the mixtures

at 0 °C to complete the oxidative polymerization of the residual aniline. The produced precipitates were separated by filtration, and washed with diluted ammonia to produce Au NPs protected by an Emeraldine base of polyaniline. The yields were more than 90 % based on the charged amount of aniline. The contents of Au were measured by atomic absorption analysis and were found to be nearly the same as the charged one.

Fabrication of hybrid films of polyaniline-protected Au nanoparticles

In order to get the hybrid films, camphorsulfonic acid (0.29 g), and polyaniline hybrid containing Au NPs prepared in situ or the mixtures of an Emeraldine base of polyaniline with PVP-protected Au NPs (0.25 g) were placed in an agate mortar and mixed with a pestle at first. After adding *m*-cresol (24.8 g), the mixture was well grinded with a pestle. The resulting mixture in a sample tube was sonicated at 50 °C for 3 h. A part of the clear supernatant was placed on a glass substrate and heated on a hot plate at 50 °C for 18 h to remove the solvent *m*-cresol. The prepared hybrid films were dried at 60 °C under vacuum.

Preparation of thiol-protected Au nanoparticles

Thiol-protected Au NPs were first prepared as follows [39]: An aqueous solution (60 mL) of $HAuCl_4\ 4H_2O$ (0.6 mmol) was at first mixed with tetraoctylammonium bromide (TOAB, 1.2 mmol) solution in toluene (20 mL). After addition of toluene (120 mL), the mixture was vigorously stirred for 24 h. The yellow aqueous layer became colorless, and the toluene layer turned orange as a result of the complex formation of $[AuCl_4]^-$ with tetraoctylammonium cations. After mixing the solution with the freshly prepared thiols, dodecanethiol (DT) or terthiophenethiol (TSH), in toluene (200 mL) for 10 min at room temperature, a freshly prepared aqueous solution (60 mL) of sodium tetrahydroborate ($NaBH_4$, 6 mmol) was added to the vigorously stirred solution. The resulting solution immediately turned from orange to black (in the case of DT) or dark green (in the case of TSH), and continued to be stirred for more than 12 h. The organic phase was then separated and subjected to complete evaporation of the solvent with a rotary evaporator. The Au NPs were re-dissolved in toluene (30 mL) and precipitated with methanol (400 mL). The particles were washed with toluene and methanol several times by centrifugation.

Fabrication of hybrid films of thiol-protected Au nanoparticles and PEDOT

In order to prepare the hybrid films of poly(3,4-ethylenedioxythiophene) (PEDOT) and Au NPs, an aqueous solution of PEDOT-poly(styrenesulfonate) (PEDOT-PSS, Aldrich) was mixed with methanol, water, and a dispersion of thiol-protected Au NPs in tetrahydrofuran (THF) at the designed volume ratios, and the mixtures were then drop-cast on glass substrates. The film sample was dried overnight at room temperature and annealed at 80 °C for 1 h. The thickness of the hybrid films was determined with a linear gage from 10 to 20 μm.

Measurements of thermoelectric properties

The temperature dependence of the electrical conductivity and the Seebeck coefficient was determined with a four-point measurement unit for thermoelectric properties for rectangular samples of the film in an electric oven at temperatures from room temperature to 443 K according to the same procedure reported [38]. The power factor was calculated from the corresponding Seebeck coefficient and electrical conductivity at a certain temperature.

Results and discussion

Hybrids of polyaniline and metal nanoparticles

At the initial stage of the research, we used PVP-protected Pt and Au NPs prepared by a conventional alcohol reduction method in the presence of PVP [22] and mixed these PVP-protected metal NPs with Emeraldine base of polyaniline prepared separately according to the literature [40] to prepare the hybrids of PVP-prepared metal NPs and polyaniline. If a large amount of PVP will be used for the

preparation of PVP-protected metal NPs, however, PVP will work as an insulator and the electrical conductivity of polyaniline will not be improved by addition of PVP-protected metal NPs. Thus, we used only a small amount of PVP (R = 0.1) to prepare the NPs. TEM images and size distribution histograms are illustrated in Fig. 9 for PVP-protected Pt (a) and Au (b) NPs at R = 0.1. The Pt NPs formed precipitates in spite of the small average particle size of 4.3 nm, while the rather large Au NPs were well dispersed.

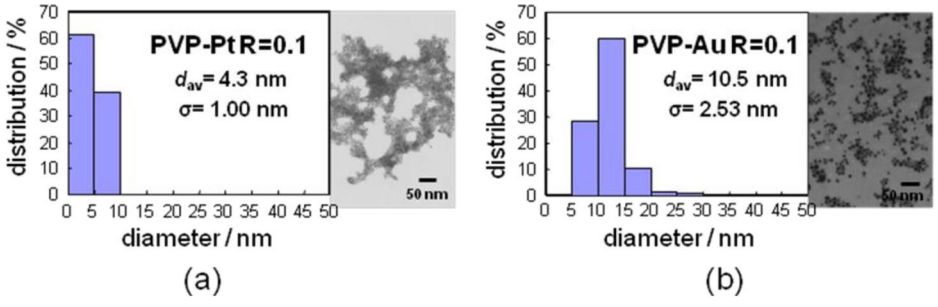

Fig. 9 TEM images and size distribution histograms of (a) PVP-protected Pt NPs and (b) PVP-protected Au NPs.

Electrical conductivities of the hybrid films of polyaniline and PVP-protected Pt and Au NPs were a little higher than the pristine polyaniline film. Results are shown in Fig. 10, depending on the charged amount of NPs. Hybrid films show about 2 times higher electrical conductivity than the pristine polaniline films, when only a small amount of metal NPs are added. When a large amount of metal NPs were added, the amount of insulating PVP added became larger in the hybrid films, which may depress the electronic current, and decrease the electrical conductivity. In fact, when large amounts of PVP were used for the preparation of metal NPs (R = 1.0) instead of R = 0.1, then the electrical conductivity of hybrid films decreased although the same amount of metal NPs were contained as shown in Fig. 11.

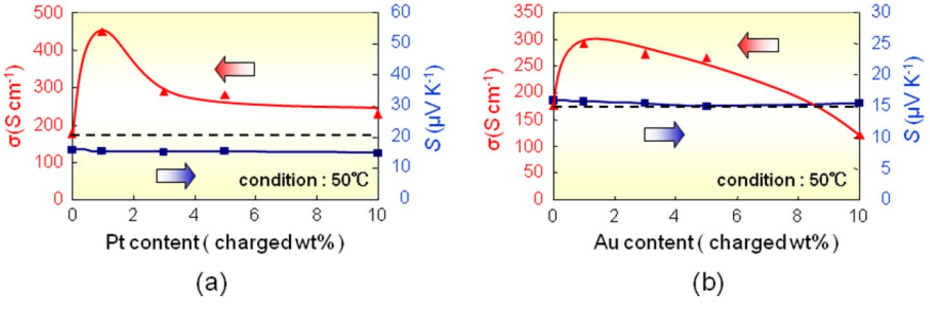

Fig. 10 Electrical conductivity and Seebeck coefficient of hybrid films of polyaniline added by PVP-protected (a) Pt NPs and (b) Au NPs.

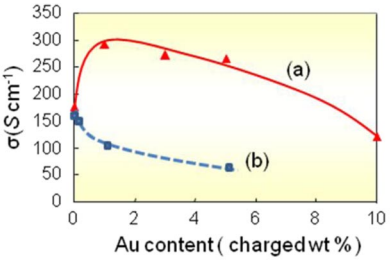

Fig. 11 Au content dependence of the electrical conductivity of hybrid films of polyaniline added by PVP-protected Au NPs. (a) $R = 0.1$, (b) $R = 1.0$.

As mentioned in the above paragraphs, the content of PVP could suppress the electrical conductivity of hybrid films. Thus, we decided to use polyaniline itself as protective colloid of metal NPs. The redox reaction between metal ions and aniline, followed by polymerization of residual aniline with an oxidant, was conducted to prepare metal NPs protected by polyaniline. Hybrid films of polyaniline and polyaniline-protected Au NPs were supplied to measure thermoelectric properties. The results are shown in Fig. 12. Although Seebeck coefficient does not charge depending on the Au content, the electrical conductivity increases rapidly with increasing Au content until ca. 1 wt %, and then decreases gradually with increasing Au content. Thus, the power factor also increases by addition of small amount of Au NPs (Fig. 12b). Thermal conductivity of conducting polyaniline film is known to be nearly the same with that of the film of insulating Emeraldine base of polyaniline [30]. Here we found that the thermal conductivity of conducting polyaniline film was not affected by hybridization with small amount of Au NPs and was kept as ca. 0.10 ± 0.03 W m^{-1} K^{-1} even after hybridization. Thus, the dimensionless thermoelectric figure-of-merit ZT of the hybrid films is ca 2.5×10^{-2}, which is ca. 2 times higher than the pristine polyaniline film (Fig. 13). In other words, the addition of a small amount of Au NPs can improve the electrical conductivity and thus ZT value of polyaniline. This is probably because Au NPs may assist the hopping of the carriers between the polyaniline molecules.

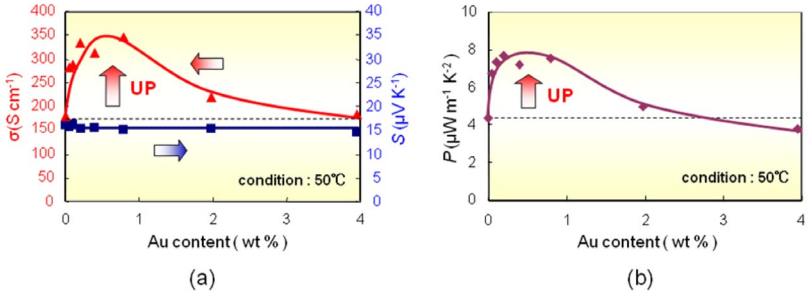

Fig. 12 Au content dependence of (a) electrical conductivity (σ) and Seebeck coefficient (S), and (b) thermoelectric power factor (P) of the hybrid films of polyaniline and polyaniline-protected Au NPs.

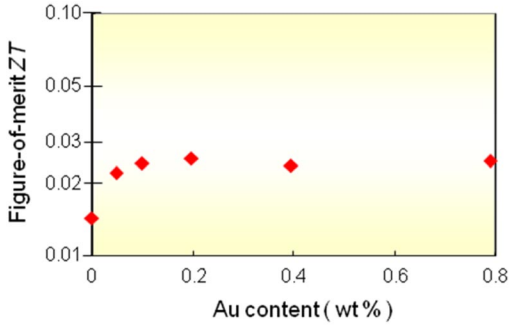

Fig. 13 Thermoelectric figure-of-merit (*ZT*) of the hybrid films of polyaniline with polyaniline-protected Au NPs depending on the Au content.

Hybrids of PEDOT and Au nanoparticles

PEDOT is known a promising conducting polymer [41]. The hybrid of PEDOT doped by PSS (PEDOT-PSS) is commercially available as an aqueous dispersion, and the drop cast of the dispersion can provide a homogeneous film. The high thermoelectric performance was reported for PEDOT tosylate films by controlling the oxidation level [35]. The thermoelectric properties of PEDOT as pressed blocks or nanofibers were also reported recently [42,43]. We have examined adding Au NPs to the PEDOT-PSS films to form hybrids in order to improve the thermoelectric performance of PEDOT-PSS.

Thiol (DT or TSH)-protected Au NPs were prepared [39], and the hybrid films were fabricated by mixing the dispersion of PEDOT-PSS and Au NPs. Interestingly, the hybridization with TSH-protected Au NPs did not improve the thermoelectric performance of the pristine PEDOT-PSS films prepared by the same method. In contrast, however, hybridization with DT-protected Au NPs made the excellent improvement even by a tiny amount (1 wt %) of Au NPs to the PEDOT-PSS films, as shown in Fig. 14 [38]. In this case, the electrical conductivity was improved from 104.2 to 240.5 S cm^{-1} at 50 °C by addition of DT-protected Au NPs, while the Seebeck coefficient was not so much improved, changing from 20.7 to 22.0 μV K^{-1}. Thus, the Au NPs may assist the hopping of the carriers between the PEDOT molecules to increase the electrical conductivity of PEDOT-PSS films, in the same way as in the case of polyaniline films.

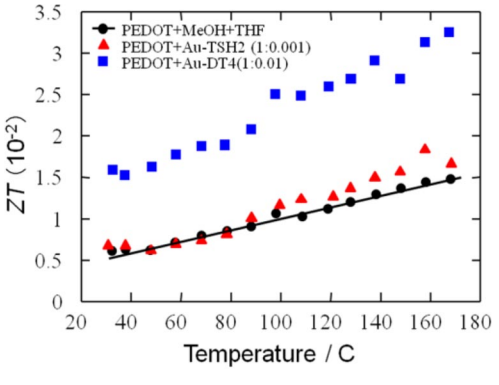

Fig. 14 Thermoelectric figure-of-merit of the pristine PEDOT-PSS films (–●–), and the hybrid films of PEDOT-PSS with TSH-protected Au NPs (▲), and DT-protected Au NPs (■).

Recently, we have found for the first time that the Au NPs can improve the Seebeck coefficient by quenching the carriers in the hybrid films of PEDOT-PSS and Au NPs [44]. Thus, metal NPs may improve the thermoelectric performance of organic thermoelectric materials of conducting polymers by improving not only the electrical conductivity but also the Seebeck coefficient.

Summary of organic thermoelectric materials

Hybridization of conducting polymers with metal NPs can improve the thermoelectric performance of organic thermoelectric materials of conducting polymers. In the case of hybrids of polyaniline with PVP-protected Pt or Au NPs, the thermoelectric performance could be improved by adding only a small amount of metal NPs, if only a small amount of PVP was used as the protectant of the NPs (R = 0.1). Since PVP is an insulator, addition of Au NPs protected by a large amount of PVP (R = 1.0) did decrease the electrical conductivity of polyaniline, and then the thermoelectric performance.

Direct hybridization of polyaniline with Au NPs, i.e., in situ preparation of polyaniline-protected Au NPs by a redox reaction, can avoid the use of insulating PVP, and the thermoelectric performance of polyaniline can be improved by using the polyaniline-protected Au NPs.

PEDOT-PSS is another promising candidate for the organic thermoelectric materials. The performance of PEDOT-PSS films can be improved by addition of Au NPs. In this case, DT was better than TSH as the protecting ligand for Au NPs. Au NPs can work as the assistant for carrier hopping (improvement of the electrical conductivity) and also as the quencher for the carriers (improvement of Seebeck coefficient).

CONCLUDING REMARKS

Energy is a big problem for human beings. Nanotechnology could offer solutions to this problem. Here, we presented two examples that could contribute to a probable solution to the energy problem. One is the electrocatalysts for polyelectrolyte fuel cells, and the other is hybrid thermoelectric materials to recover electrical energy from exhaust heat.

Polyelectrolyte fuel cells are a promising system to get electricity for fossil fuels at high conversion efficiency. The issue of the cost of the Pt electrocatalysts must be solved for the polyelectrolyte fuel cells to be practically used. Here, we proposed PFSA-protected Pt and AuPt bimetallic NPs as the electrocatalyst. The formation of nanonetwork and Au-core/Pt-shell structure can reduce the amount of Pt used for the electrocatalyst. These specific properties of PFSA-protected Pt and AuPt bimetallic NPs are the advantages to construct practical membrane electrode assemblies from the viewpoints of the processing and the cost of the polyelectrolyte fuel cells.

Pt and Au NPs can also be used for fabrication of hybrid films for organic thermoelectric materials. Organic thermoelectric materials of conducting polymer have several advantages compared with the conventional thermoelectric materials of inorganic semiconductors. Low cost based on the resource price and printing processing, and high flexibility and large device area based on organic polymers are the examples. The addition of a small amount of Pt or Au NPs can improve the thermoelectric performance of organic materials, although some sophisticated design could be necessary for the high performance. We could successfully demonstrate how to improve the electrical conductivity of conducting polymer by adding a small amount of metal NPs. It should be emphasized that addition of metal NPs to conducting polymers can improve the thermoelectric performance by increasing not only the electrical conductivity but also the Seebeck coefficient [44].

Metal NPs can be prepared by various elements and in various structures. Multimetallic alloy NPs also can be fabricated recently. These various metal NPs may serve to solve the energy problem. The speed of the development and application of this science and technology will depend on further original new ideas.

ACKNOWLEDGMENTS

The author thanks the co-workers, especially Dr. H. Naohara, Mr. T. Yoshimoto, and Mr. Y. Okamoto, for the electrocatalyst works, and Dr. N. Jiravanichanun and Mr. H. Marutani for the hybrid thermoelectric materials works. Financial support from the Toyota Motor Corporation and the Ministry of Education, Culture, Sports, Science, and Technology (MEXT), Japan (Grant-in-Aid for Scientific Research (B) No. 21310077 and Yamaguchi Green Materials Cluster) are also acknowledged.

REFERENCES

1. C. B. Murray, C. R. Kagan, M. G. Bawendi. *Ann. Rev. Mater. Sci*. **30**, 545 (2000).
2. S. Link, M. A. El-Sayed. *J. Phys. Chem. B* **103**, 8410 (1999).
3. B. Corain, G. Schmid, N. Toshima (Eds.). *Metal Nanoclusters in Catalysis and Materials Science: The Issue of Size Control*, Elsevier, Amsterdam (2008).
4. M. Z. Jacobson. *Energy Environ. Sci*. **2**, 148 (2009).
5. M. Conte, P. Prosini, S. Passeriro. *Mater. Sci. Eng., B* **108**, 2 (2004).
6. B. C. H. Stede, A. Heinzel. *Nature* **414**, 345 (2001).
7. T. E. Springer, T. A. Zawodzinski, S. Gottesfeld. *J. Electrochem. Soc*. **138**, 2334 (1991).
8. A. S. Arico, P. Bruce, B. Scrosati, J. M. Tarescon, W. van Schalkwijk. *Nat. Mater.* **4**, 366 (2005).
9. R. Venkatasubramanian, E. Siivola, T. Colpitts, B. O'Quinn. *Nature* **413**, 597 (2001).
10. I. Terasaki, Y. Sasago, K. Uchinokura. *Phys. Rev. B* **56**, R12685 (1997).
11. L. D. Hicks, M. S. Dresselhaus. *Phys. Rev. B* **47**, 12727 (1993).
12. A. I. Hochbaum, R. K. Chen, R. D. Delgado, W. J. Liang, E. C. Garnett, M. Najarien, A. Najundar, P. D. Yang. *Nature* **451**, 163 (2008).
13. G. J. Snyder, E. S. Toberer. *Nat. Mater.* **7**, 105 (2008).
14. H. A. Gasteiger, S. S. Kocha, B. Sompalli, F. T. Wagner. *Appl. Catal., B* **56**, 9 (2005).
15. U. A. Paulus, A. Wokaun, G. G. Scherer, T. J. Schmidt, V. Stameukovic, V. Radmilovic, N. M. Matkovic, P. N. Ross. *J. Phys. Chem. B* **106**, 4181 (2002).
16. T. Toda, H. Igarashi, M. Watanabe. *J. Electroanal. Chem*. **460**, 258 (1999).
17. N. M. Markovic, T. J. Shmidt, V. Stementivic, P. N. Ross. *Fuel Cells* **1**, 105 (2001).
18. Y. Shao, G Yiu, Z. Wang, Y. Gao. *J. Power Sources* **167**, 235 (2007).
19. H. Naohara, Y. Okamoto, N. Toshima. *J. Power Sources* **196**, 7510 (2011).
20. N. Toshima, H. Naohara, T. Yoshimoto, Y. Okamoto. *Chem. Lett*. **40**, 1095 (2011).
21. H. Naohara, T. Yoshimoto, N. Toshima. *J. Power Sources* **195**, 1051 (2010).
22. H. Hirai, Y. Nakao, N. Toshima. *J. Macromol. Sci., Chem. A* **13**, 727 (1979).
23. K. Esumi, A. Suzuki, A. Yamahira, K. Torigoe. *Langmuir* **16**, 2604 (2000).
24. H. Zhang, M. Okumura, N. Toshima. *J. Phys. Chem. C* **115**, 14883 (2011).
25. N. Toshima, M. Harada, T. Yonezawa, K. Kushihashi, K. Asakura. *J. Phys. Chem*. **95**, 7448 (1991).
26. Y. Mizukoshi, T. Fujimoto, Y. Nagate, R. Oshima, Y. Maeda. *J. Phys. Chem. B* **104**, 6028 (2000).
27. T. Yonezawa, N. Toshima. *J. Mol. Catal.* **83**, 167 (1993).
28. N. Toshima, T. Yonezawa. *New J. Chem*. **22**, 1179 (1998).
29. T. Ishida, M. Haruta. *Angew. Chem., Int. Ed.* **46**, 7154 (2007).
30. H. Yan, N. Toshima. *Chem. Lett*. 1217 (1999).
31. H. Yan, N. Sada, N. Toshima. *J. Therm. Anal. Calorim.* **69**, 881 (2002).
32. H. Yan, T. Ohta, N. Toshima. *Macromol. Mater. Eng*. **287**, 139 (2001).
33. N. Toshima. *Macromol. Symp*. **186**, 81 (2002).
34. Y. Hiroshige, M. Ookawa, N. Toshima. *Synth. Metals* **157**, 467 (2007).
35. O. Bubnova, Z. U. Khan, A. Malti, S. Braun, M. Fahlman, M. Borggren, X. Crispin. *Nat. Mater*. **10**, 429 (2011).

36. D. Kim, Y. Kim, K. Choi, J. C. Grumlan, C. H. Yu. *ACS Nano* **4**, 513 (2010).
37. N. Toshima, M. Imai, S. Ichikawa. *J. Electron. Mater*. **40**, 989 (2011).
38. N. Toshima, N. Jiravanichanun, H. Marutani. *J. Electron. Mater*. **41**, 1735 (2012).
39. T. Teranishi, S. Hasegawa, T. Shimizu, M. Miyake. *Adv. Mater*. **13**, 1699 (2001).
40. P. N. Adams, P. J. Langhlin, A. P. Monkman. *Polymer* **37**, 3411 (1996).
41. S. Kirchmeyer, K. Reuter. *J. Mater. Chem*. **15**, 2077 (2005).
42. F.-X. Jiang, J.-K. Xu, B.-Y. Lu, Y. Xie, R.-J. Huang, L.-F. Li. *Chin. Phys. Lett*. **25**, 2202 (2008).
43. D. K. Taggart, Y. Yang, S.-C. Kung, T. M. Mcintire, R. M. Penner. *Nano Lett*. **11**, 125 (2011).
44. N. Toshima, N. Jiravanichanun. *J. Electron. Mater*. In press. http://dx.doi.org/10.1007/s11664-012-2458-y

